Urban Climate 25 (2018) 135–151

Contents lists available at ScienceDirect

Urban Climate

journal homepage: www.elsevier.com/locate/uclim

The effects of increasing surface reflectivity on heat-related mortality in Greater Montreal Area, Canada

Zahra Jandaghian, Hashem Akbari*

Heat Island Group, Building, Civil and Environmental Engineering Department, Concordia University, Montreal, Canada

ARTICLE INFO

Keywords:
Heat-related mortality
Weather research and forecasting model
Urban canopy model
Spatial synoptic classification
Increasing surface reflectivity

ABSTRACT

Heat-related mortality is increasing as the result of climate change, extreme heat events and higher ambient temperature because of urban heat island (UHI) phenomenon. We coupled the Weather Research and Forecasting model (WRFV3.6.1) with a multi-layer of the Urban Canopy Model (ML-UCM) to investigate the effects of UHI intensity during the 2005 and 2011 heat wave periods in Greater Montreal Area (GMA), Canada. Each day of simulation is categorized into an air mass type using the Spatial Synoptic Classification. Using the non-accidental mortality data during summer period, the number of deaths above the expected mean anomalous daily mortality is calculated for each air mass classification. Results indicate that moist tropical plus and dry tropical weather have the highest rank in heat-related death. We assessed the effects of increasing surface reflectivity (ISR) on four meteorological parameters: 2-m air temperature, 10-m wind speed, 2-m relative humidity, dew point temperature, and four heat stress indices: National Weather Service – Heat Index, Apparent Temperature, Canadian Humid Index, and Discomfort Index (DI). ISR decreased air temperature by 0.6 °C, increased relative humidity by 2%, increased dew point temperature by 0.4 °C. The DI improved by 3% and heat-related mortality decreased by nearly 3.2% during heat wave periods in GMA.

1. Introduction

Heat-related mortality can be magnified in urban areas because of the urban heat island effects. The climate change can also exacerbate the extreme heat events and the intensity, frequency and duration of UHI (IPCC, 2014). UHI intensity and duration cause an increase in morbidity and mortality (Nitschke et al., 2011; Wang et al., 2012; Jenkins et al., 2014; Horton et al., 2014; Hajat et al., 2010; Harlan et al., 2006; Harlan and Ruddell, 2011). Health impacts range from heat exhaustion to heat stress, kidney failure and heart attacks (WHO, 2010; Matzarakis and Nastos, 2011). Heat-related mortality occurs mostly for vulnerable sections of the society as elderly, homeless, and socially disadvantaged people (Vandentorren et al., 2006; Vaneckova et al., 2010; Peng et al., 2011; Cusack et al., 2011; Yardley et al., 2011; Oliver et al., 2015). Much of the excess mortality is related to cardiovascular, cerebrovascular and respiratory causes and is concentrated in the elderly (Åström et al., 2011; Bunker et al., 2016).

Epidemiological and statistical studies indicated a positive correlation between extreme ambient temperature and mortality during summer time within elderly particularly among women (Mcgeehin and Mirabelli, 2001; Diaz et al., 2002; O'Neill et al., 2003, 2005; O'Neill and Ebi, 2009). People living in urban environments are at greater risk than those in rural areas (Diaz et al., 2002), whereby inner urban environments, with high thermal mass and low ventilation, absorb and retain heat and can amplify the rise in

* Corresponding author at: Urban Heat Island Group, Building, Civil and Environmental Engineering Department, Concordia University, 1455, de Maisonneuve Blvd. West, EV006.409, Montreal, Quebec H3G 1M8, Canada.
E-mail addresses: z_janda@encs.concordia.ca (Z. Jandaghian), Hashem.Akbari@Concordia.ca (H. Akbari).

https://doi.org/10.1016/j.uclim.2018.06.002
Received 10 November 2017; Received in revised form 30 April 2018; Accepted 17 June 2018

temperature. Anderson and Bell (2009) estimated an increment in death by 4.5% per degree Celsius in heat wave intensity and 0.4% per day in heat wave duration. Zanobetti and Schwartz (2008) and Zanobetti et al. (2014) used mortality data across the United States and found out that mortality increases by 3.6% per °C increase in temperature. Basu (2009) and Basu and Samet (2002) evaluated the relationship between the mortality rate and temperature and found that mortality rate increased 4.6% per °C rise in apparent temperature. Mcmichael et al. (2006) presented the results of an investigation on the relation between temperature and mortality in eleven cities of eastern United States. They defined a U-Shaped relation between number of daily deaths and daily temperature and illustrated that mortality rates rise as temperatures reach beyond the upper and lower thresholds of human comfort.

Air temperature in urban area is typically higher than that of the surroundings. In addition, because of climate change, the extreme heat waves are becoming more frequent, prolonged and severe. The combination of these two phenomena leads to higher day-time temperatures, causing heat stress for urban dwellers. The extreme heat events analyses indicated that UHI plays an important role in premature urban mortality (Conti et al., 2005); hence signifying the importance of the UHI characterization on air temperature, humidity, wind speed, radiation, and air pollution (Fischer et al., 2012). The indirect effect of UHI is to increase cooling energy demand in summer time and increase photochemical reaction rates, thus worsen air quality. The adverse impacts of air pollution on human health should also be considered, which is beyond the scope of this study.

The effects of UHI and extreme heat events can be evaluated by numerical simulations. Several numerical modeling studies investigated the effects of only temperature during heat wave period (Diffenbaugh and Ashfaq, 2010), but few considered the combination effects of temperature and humidity (Sherwood and Huber, 2010; Smoyer et al., 2000). Increasing surface reflectivity is a verifiable, measurable, and repeatable mitigation strategy to fight the impacts of UHI in regional, urban and global scales (Akbari et al., 2001, 2009; Arnfield, 2003; Ban-Weiss et al., 2014; Taha, 2008, 2009; Taha, 1997). Akbari and Touchaei (2014) and Akbari and Kolokotsa (2016) indicated that the albedo of most surfaces in urban areas, whether as roofs or pavements, range from 0.1 to 0.2, but it can be even higher due to the use of different materials in cities` structure. Taha (1997) considered the impacts of surface albedo, evapotranspiration, anthropogenic heating, and presented that increasing the albedo by up to 0.15 can reduce summertime temperatures in the urban area of Los Angeles by up to 1.5 °C. Jandaghian et al. (2017) showed that by increasing surface albedo during a rainy episode in summer 2009, air temperature decreases by 0.2 °C, wind speed slightly increases, relative humidity and precipitation respectively decrease by 2.8% and 0.2 mm over GMA.Jandaghian and Akbari (2018) also showed that increasing surface albedo in Sacramento, Houston and Chicago result in a decrease in air temperature by 2.3 °C in urban areas and 0.7 °C in suburban areas; a slight increase in wind speed; an increase in relative humidity (3%) and dew point temperature (0.3 °C); a decrease of $PM_{2.5}$ and O_3 concentrations by 2.7 $\mu g/m^3$ and 6.3 ppb in urban areas and 1.4 $\mu g/m^3$ and 2.5 ppb in suburban areas, respectively. Akbari et al. (2009) and Oleson et al. (2010 and 2011) simulated the energy saving aspect of highly reflective surfaces on a global scale. Jacobson and Ten Hoeve (2012) used a global model to analyze the effect of urban surfaces and white roofs on global and regional climate. Increasing solar reflectance of pavements are currently employed in several cities across globe (Chip seals in San Jose, California; Grass-Crete in Singapore and Osaka, Japan) (Akbari and Kolokotsa, 2016). The cool pavement strategy reduces the urban temperature and thus cooling energy demands in buildings by 2% in Greater Montreal Area (Touchaei and Akbari, 2015). Successful implementation of cool pavements depends on many factors (such as its materials and life-cycle cost performance) that need to be considered (Akbari and Kolokotsa, 2016).

Here, the first intention is to simulate the impacts of extreme heat events on meteorological parameters and heat-related death over the Greater Montreal Area during two heat wave periods in 2005 and 2011. We applied the fully coupled online Weather Research and Forecasting model (WRFV3.6.1) with a multi-layer of the Urban Canopy Model (ML-UCM). We evaluated the model performance by comparing the meteorological parameters: 2-m air temperature, 10-m wind speed, 2-m relative humidity, dew point temperature with measurements obtained from four weather stations over the domain. The second objective is to assess the effects of increasing surface reflectivity (ISR) on aforementioned meteorological parameters and four indices of heat stress: National Weather Service – Heat Index (NWS-HI), Apparent Temperature (AP), Canadian Humid Index (CHI), and Discomfort Index (DI). Another focus is to analyze the effects of ISR on air mass type modifications and heat-related death. Each day of simulation is classified into an air mass type category. Then, the number of deaths above the expected mean anomalous daily mortality is calculated within each classification.

We limited our analysis *only* to the effects of surface albedo enhancement on aforementioned parameters and heat-related mortality and did not consider the pedestrian thermal comfort. The evaluation of day-time pedestrian thermal comfort level depends on using sky-view factor (SVF) as an indicator of the complexity of urban geometry, street orientation and winds pattern (Kruger et al., 2010). Hong and Lin (2014) used simulation platform for outdoor thermal environment and concluded that building layout pattern and trees arrangement have significant effects on the wind pattern and thus pedestrian thermal comfort. Another factor in such estimation is solar radiation loads.Although, understanding these factors is essential in terms of heat-related morbidity, but it is beyond the scope of present study.

2. Methodology

2.1. Air mass classification and heat related mortality

A wide range of weather metrics are used to investigate the heat-health relationship such as temperature, relative humidity, solar radiation, barometric pressure, and wind speed (Barnett et al., 2010; Zhang et al., 2014a & b). The Spatial Synoptic Classification (SSC; Sheridan, 2002) was developed based on a set of meteorological conditions (i.e., air temperature, dew point temperature, air pressure, wind speed, cloud cover) to place each day into a specific air mass type for the particular location and time of year. The SSC

Table 1
Summertime mortality rate for GMA within five weather types (1981–2000): weather type frequency for JJA and relative mortality (the averaged anomalous number of heat-related death above baseline value for mean daily mortality) [Mortality rate per 100,000 people, calculated based on Statistics Canada 2011 Census as 3,824,221 people in GMA].

Synoptic category	Frequency (%)	Mortality
DM	32.2	1.96
DT	1.3	2.27
MM	24.0	1.95
MT	22.0	2.13
MT+	4.4	2.38

Dry Moderate (DM): mild and dry air; Dry Tropical (DT): the hottest and driest conditions; Moist Moderate (MM): warmer and more humid conditions; Moist Tropical (MT): warm and very humid; Moist Tropical Plus (MT+): hotter and more humid subset of MT (Sheridan, 2002).

has been used in several human health-climate studies (e.g., Kalkstein et al., 2013; Hajat et al., 2010; Hanna et al., 2011; Vanos et al., 2013, 2014; Sheridan et al., 2009). Statistical studies determine that “oppressive air masses” such as Dry Tropical (DT), Moist Tropical (MT), and Moist Tropical Plus (MT+) are associated with increasing heat-related mortality (Kalkstein et al., 2011).

As this research focuses on heat, the summer period of June, July and August (JJA) in Greater Montreal Area (GMA) is being analysed. In another study, Vanos et al. (2014) classified weather types into SSC for 12 cities in Canada. They defined the summertime statistics of GMA within synoptic weather type categories. The meteorological data applied to classify weather types into SSC was collected from airport weather stations maintained by the Meteorological Service of Canada.

To estimate heat-related mortality, the daily non-accidental mortality data was collected across the city's metropolitan area from the Canadian Vital Statistics data bases at Statistics Canada over 20 years (1981–2000). These mortality data were then standardized to account for demographic changes in the population characteristics, such as aging and growth, or even a decrease in the overall death due to people's immigration to rural areas for vacations and holidays in summer (Kalkstein and Sheridan, 2003). Thus, for standardization, first the mean mortality for each day in summer was considered for the 20-year period, and a trend line was fit to these data. Then, the anomalous mortality was identified as a value above or below the established trend lines for each day during this period. Table 1 represents the GMA specific air mass classification, the summertime frequencies (JJA, %), and heat-related mortality (Vanos et al., 2014; Martel et al., 2010). Here, the number of deaths related to each air mass classification, is estimated based on the rate above the mean anomalous daily mortality in Montreal per 100,000 people. The Statistics Canada Census estimated the population of Montreal as 3,824,221 people in 2011.

The Dry Moderate (DM) weather type, that includes mild and dry air in the summer season, is the most common type in the Greater Montreal Area. The highest rate of mortality in GMA during summer periods corresponds to the hotter and more humid air mass type [MT+], while the dry tropical condition [DT] places second (Vanos et al., 2014).

2.2. Meteorological simulations

The NCAR Weather Research and Forecasting Model (WRFV3.6.1) (Skamarock et al., 2008) is applied within a multi-layer of the Urban Canopy Model (ML-UCM) (Chen et al., 2011) to simulate the meteorological interactions in the atmosphere. WRF is a non-hydrostatic mesoscale numerical weather prediction (NWP) system. The Advanced Research WRF is a dynamic solver that the equations are formulated using a terrain-following hydrostatic-pressure vertical coordinate. Reynolds-Averaged Navier-Stokes equations (RANS) are solved on a horizontal and vertical grid to represent the evolution of the state of the atmosphere (Skamarock et al., 2008). Atmospheric motions are determined between the model variables due to the external forcing, such as solar radiation, and interactions with the Earth's surface, including fluxes of heat, moisture and momentum. Different schemes are available for microphysics, cumulus parameterization, surface and atmospheric radiations and boundary layers (WRF User's Guide, 2016).

2.2.1. Numerical domain and simulation episodes

Montreal is the second largest city in Canada and is centered at the ~45.5° N and ~73.6° W. The horizontal domain of the simulations is composed of four two-way nested domains with 37 × 22, 43 × 34, 91 × 61, and 145 × 91 grid points, and a grid spacing of 9, 3, 1 and 0.333 km x km, respectively. The simulations were conducted with the initial and boundary conditions obtained from the North American Regional Reanalysis (NARR) (Mesinger et al., 2006) with a grid resolution of 32 km and a time resolution of 3-h. Here, a vertical resolution of 51eta level is defined to take full advantages of the urban parameterizations. Land Use/Land Cover (LULC) data was derived from the USGS 24-category data set. Advanced Very High-Resolution Radiometer (AVHRR) measures the background surface albedo (Csiszar and Gutman, 1999). Fig. 1 shows the simulation domain and Land Use Land Cover of the 4th domain including GMA.

The 2005 heat wave event occurred from 10th through 12th of July. The precipitation was 15 mm on the 9th of July and the next day, a humid and high temperature condition captured inhabitants by surprise. (Environment Canada, 2017). The temperature increased from 23 °C at 2 a.m. to 33 °C at 2 p.m. on the 12th, a cloud cover of 10% was recorded. The 2011 Montreal heat wave event

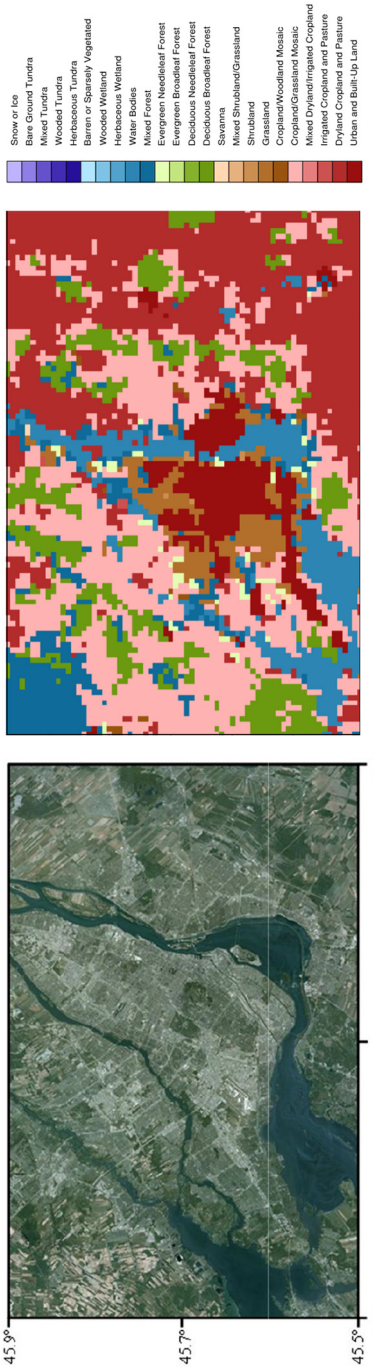

Fig. 1. Simulation domain (http://maps.google.ca) and Land Use Land Cover (LULC) of GMA; black color shows the urban area

occurred from 17th through 23rd of July. The maximum temperature was as high as 36 °C and there was no precipitation and cloud coverage before or after this period. The 2011 heat wave period started from eastern Ontario on July 17th and reached to 36 °C across the province of Quebec on July 21 and continued across US (National Climate Data Center- NOAA; Historical Climate Data- Canada). Accordingly, the simulation episodes are defined based on these two heat wave events in Greater Montreal Area in 2005 and 2011. One simulation is during the heat wave period in 2005, from the 9th to 12th of July (The highest recorded temperature being 33 °C on the 11th), and the other one is during the peak of the heat wave event, from 20th to 23rd of July 2011 (The highest recorded temperature being 36 °C on the 21st). Each simulation begins at 1200 UTC (LST = UTC - 4 h) of the previous day of each period and finishes at the 1200 UTC of a day after. The first 24 h considered as the spin up of the simulations.

2.2.2. Meteorological simulation setup

To analyze the urban characteristics and evaluate the local climate phenomena as the urban heat island, it is essential to have a careful selection of surface, radiation and boundary layer physics in WRF. The community land-surface model NOAH-LSM provides skin temperature, surface sensible and latent heat fluxes as lower boundary conditions for the meteorological model. The planetary boundary layer is simulated by the Mellor-Yamada-Janjic scheme (Janjic, 1994, 2002) using Eta similarity theory (Janjic, 2002). We used Rapid Radiative Transfer Model (RRTMG; Iacono et al., 2008), Lin scheme (Lin et al., 1983; Lin and Colle, 2011), and Grell 3D (Grell and Devenyi, 2002) as radiation, microphysics and cumulus models, respectively. We coupled the simulation with a multilayer of the Urban Canopy Model (ML-UCM) to estimate heat and moisture fluxes (Chen and Dudhia, 2001). We activated the positive-define advections of moisture, scalars and turbulent kinetic energy to maintain model stability.

2.3. Increasing surface reflectivity

The base condition (hereafter referred to as CTRL) and increasing surface reflectivity (hereafter referred to as ALBEDO) are the two scenarios used here. ALBEDO differs from CTRL in the surface reflectivity that increase all over the domain in the urban areas. In the CTRL case, the albedo of roofs, walls, and grounds are assumed to be 0.2, while in ALBEDO, the reflectivity of these surfaces increased by 0.65, 0.60, and 0.45, respectively. The practical drawback of high albedo pavement is its glare that may affect the pedestrian's eyesight. Increasing the reflectivity of pavement by 0.25 is considered as a value that causes no glare problem and has been tested in other similar studies in Greater Montreal Area, Canada (Touchaei and Akbari, 2013; Touchaei and Akbari, 2015, Jandaghian et al., 2017). Here, three urban land-use categories are defined: low-intensity residential, high-intensity residential and industrial and commercial. To improve the estimate of energy exchange between the interior of buildings and the outdoor atmosphere, the multilayer of the Urban Canopy Model (ML-UCM) and indoor-outdoor exchange model of Building Energy Model (BEM) are coupled within the WRF (Chen and Dudhia, 2001).

3. Results

3.1. Model performance evaluation

The meteorological parameters: 2-m air temperature (T2), 10-m wind speed (WS10), 2-m relative humidity (RH2) and dew point temperature (DPT) of CTRL results are analysed and compared with the measurements obtained from urban and rural weather stations across the domain. The set of metrics calculation applied for these evaluations are:Mean Bias Error (MBE), Mean Absolute Error (MAE) and Root Mean Square Error (RMSE) (Jandaghian et al., 2017). The urban weather stations are McTavish (MT) and Pierre Elliott Trudeau Intl (PET). The rural weather stations are Montreal/St-Hubert (SH) and Ste-Anne-de-Bellevue (SAB). Table 2 represents their geographical locations.

Table 3 represents the maximum air temperature measured in weather stations for the 2005 and 2011 heat wave periods during three consecutive days in July. The hourly data obtained from weather stations are compared with the hourly simulated values for CTRL case simulations. Table 4 represents the MBE, MAE and RSME of aforementioned parameters. Fig. 2 shows comparisons between simulated and observed 2-m air temperature, 10-m wind speed, and dew point temperature in four weather stations and 2-m relative humidity for urban and rural areas.

The model, on average, slightly overestimates the air temperature, wind speed and dew point temperature in the 2005 simulation, and slightly underestimates the air temperature and wind speed in the 2011 simulation. One of the reason is that the effects of micro scale parameters cannot be captured in mesoscale models precisely. The heat emission from buildings and the transportation sectors is miscalculated in model estimation. There is another possibility that the position of weather stations effects the wind speed

Table 2
Weather stations in Greater Montreal Area with their locations (Latitude, Longitude, and Elevation).

Station Name	Station Code	Latitude (N)	Longitude (W)	Altitude asl (m)
McTavish	MT	45.500	−73.580	72.8
Pierre Elliott Trudeau	PET	45.470	−73.750	36.0
St-Hubert	SH	45.520	−73.420	27.4
Ste-Anne-de-Bellevue	SAB	45.430	−73.930	39.0

Table 3
Max air temperature measured in four weather stations over GMA in 2005 and 2011heat wave periods.

Heat wave periods	July 2005	Max temperature (°C)			
		MT	PET	SH	SAB
July 2005	10th	31.6	31.5	31.1	30.8
	11th	32.3	32.8	31.5	32.2
	12th	30.6	30.6	30.7	30.3
	July Average T (°C)	**26.9**	**27.3**	**27.0**	**27.1**
July 2011	21th	34.9	35.6	36.0	34.7
	22nd	31.3	31.9	32.6	32.2
	23rd	31.6	32.6	32.6	31.9
	July Average T (°C)	**28.3**	**28.5**	**29.0**	**28.5**

Table 4
MBE, MAE, and RSME of 2-m air temperature (°C), 10-m wind speed (km/h) and dew point temperature (°C) simulation results in CTRL case vs. measurements obtained from weather stations over the domain in 2005 and 2011.

Station Code	2-m air temperature (°C) in 2005			2-m air temperature (°C) in 2011		
	MBE	MAE	RMSE	MBE	MAE	RMSE
MT	0.08	1.50	1.76	0.07	1.51	1.91
PET	−0.62	1.20	1.44	−0.88	1.37	1.83
SH	0.02	1.19	1.50	−0.94	1.30	1.70
SAB	1.07	1.28	1.65	0.03	1.10	1.47
Average	0.12	1.25	1.53	−0.43	1.32	1.73
Station Code	10-m wind speed (km/h) in 2005			10-m wind speed (km/h) in 2011		
	MBE	MAE	RMSE	MBE	MAE	RMSE
MT	1.66	1.82	2.30	−0.61	0.85	0.91
PET	−0.63	1.88	2.11	−2.17	2.25	2.40
SH	−0.13	2.38	2.21	−2.83	3.11	2.11
SAB	0.54	1.88	2.11	−0.33	1.25	2.81
Average	0.36	1.99	2.18	−0.93	1.86	2.05
Station Code	Dew point temperature (°C) in 2005			Dew point temperature (°C) in 2011		
	MBE	MAE	RMSE	MBE	MAE	RMSE
MT	0.82	0.83	0.90	0.52	0.58	0.71
PET	0.33	0.55	0.61	0.71	0.74	0.91
SH	−0.19	0.51	0.61	0.47	0.48	0.61
SAB	−0.16	0.38	0.52	0.93	0.93	1.01
Average	0.21	0.56	0.44	0.65	0.68	0.81

measurements, especially when they are in the urban canopy and close to city centers and skyscrapers. The relative humidity at the 2-m height is estimated based on a calculation in National Oceanic and Atmospheric Administration (NOAA) weather services.

Jandaghian et al. (2017) run a sensitivity analysis of physical parameterizations in WRF for urban climate simulations in Greater Montreal Area for 3 consecutive days in 2009. The results indicated the mean absolute error (MAE) of the 2-m air temperature, wind speed, relative humidity, and precipitation are approximately 1.4 °C, 1 m/s, 16% and 2 mm, respectively. In other studies, the comparison of thermal components of WRF and the Fifth-Generation NCAR/Penn State Mesoscale Model (MM5) indicated that both models have the MBE of T2 as almost −3.8 °C to 0.2 °C during a year. (Gilliam et al., 2006; Wu et al., 2008; Wang et al., 2009; Liu et al., 2010). Thus, the performance of WRF is generally consistent with the measurements and the results are well reliable for further investigations.

3.2. Measures of heat stress indices

Human thermal comfort depends on ambient temperature, relative humidity, wind speed and behavioral factors, for instance metabolic rate and clothing level (Epstein and Moran, 2006). Heat indices are defined to indicate individual's thermal comfort. We estimated four heat stress indices based on environmental variables, (e.g. temperature and relative humidity) as follows: National Weather Service – Heat Index (NWS-HI), Apparent Temperature (AP), Canadian Humid Index (CHI), and Discomfort Index (DI). The National Weather Service–Heat Index (NWS-HI) is calculated based on air temperature and relative humidity (%). Apparent Temperature (AT) (Eq. (1)) is the air temperature at a specific humidity ratio (Kalkstein and Valimont, 1986).

$$AT = 23.2 + 0.55T2 + 0.003DPT^2 - 0.2DPT \quad (1)$$

where $T2$ is 2-m air temperature and DPT is dew point temperature in °C. The Canadian Humid Index (CHI) (Eq. (2)) considers the

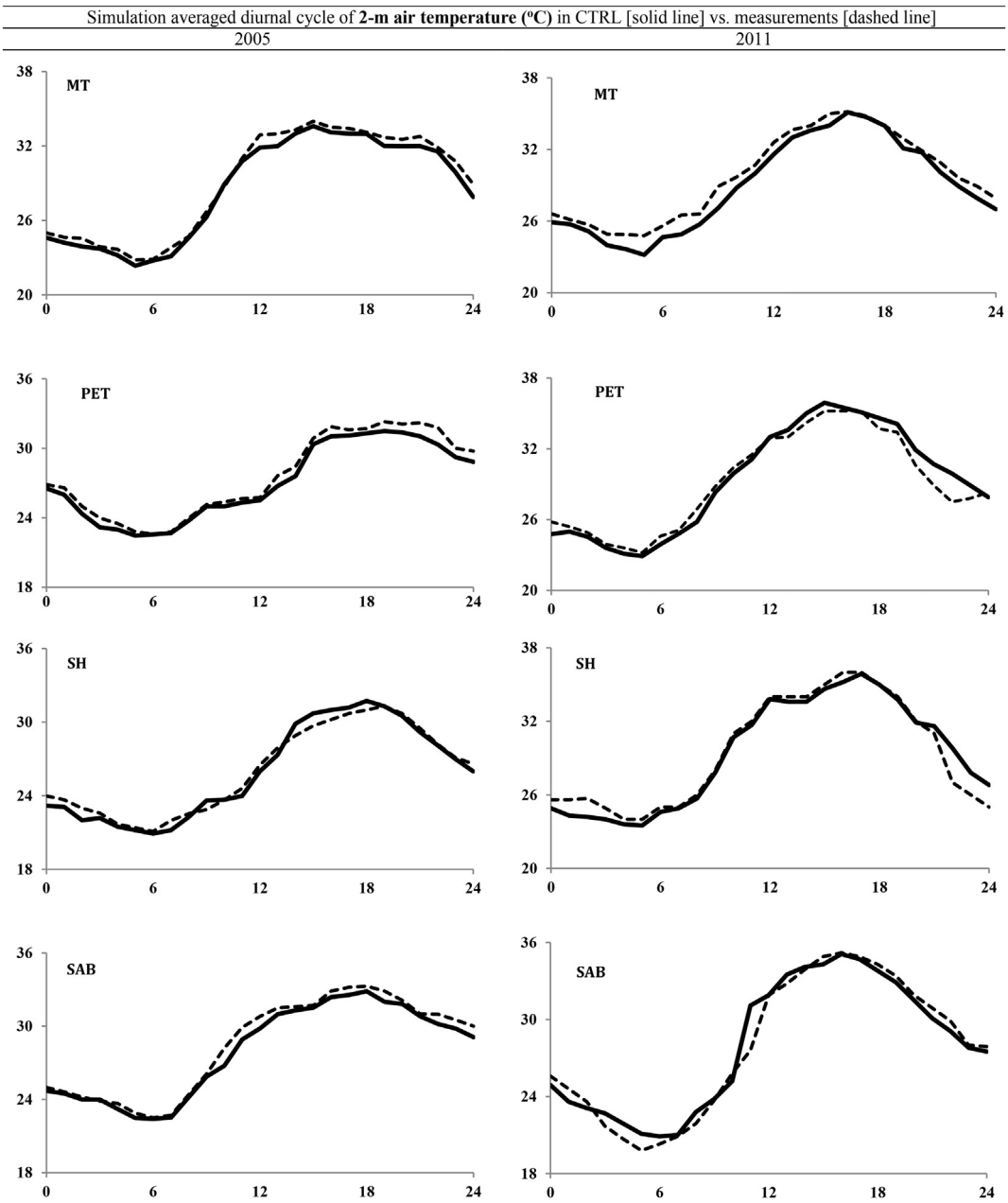

Fig. 2. Simulatied averaged diurnal cycle of 2-m air temperature (˚C), 10-m wind speed (km/h), dew point temperature (˚C), 2-m relative humidity (%) in CTRL [solid line] vs. measurements [dashed line] from four weather stations over GMA during 2005 [left] and 2011 [right] heat wave periods.

combination of two important meteorological factors, air temperature and vapor pressure, as one number to reflect how very hot and humid weather feels to an average person.

$$CHI = T2 + (0.55 \times (VP - 10)) \quad (2)$$

where VP is the vapor pressure in mille-bars (mb). The Discomfort Index (DI) (Eq. (3)) evaluates the human heat threshold due to air temperature and relative humidity. The higher DI indicates the higher value of discomfort.

$$DI = T2 - (0.55 \times (1 - 0.01RH)) \times (T2 - 14.5) \quad (3)$$

Fig. 3 shows the simulation results of an averaged diurnal (3-day) cycle of these parameters over GMA during the 2005 and 2011 heat wave periods in urban and rural areas.

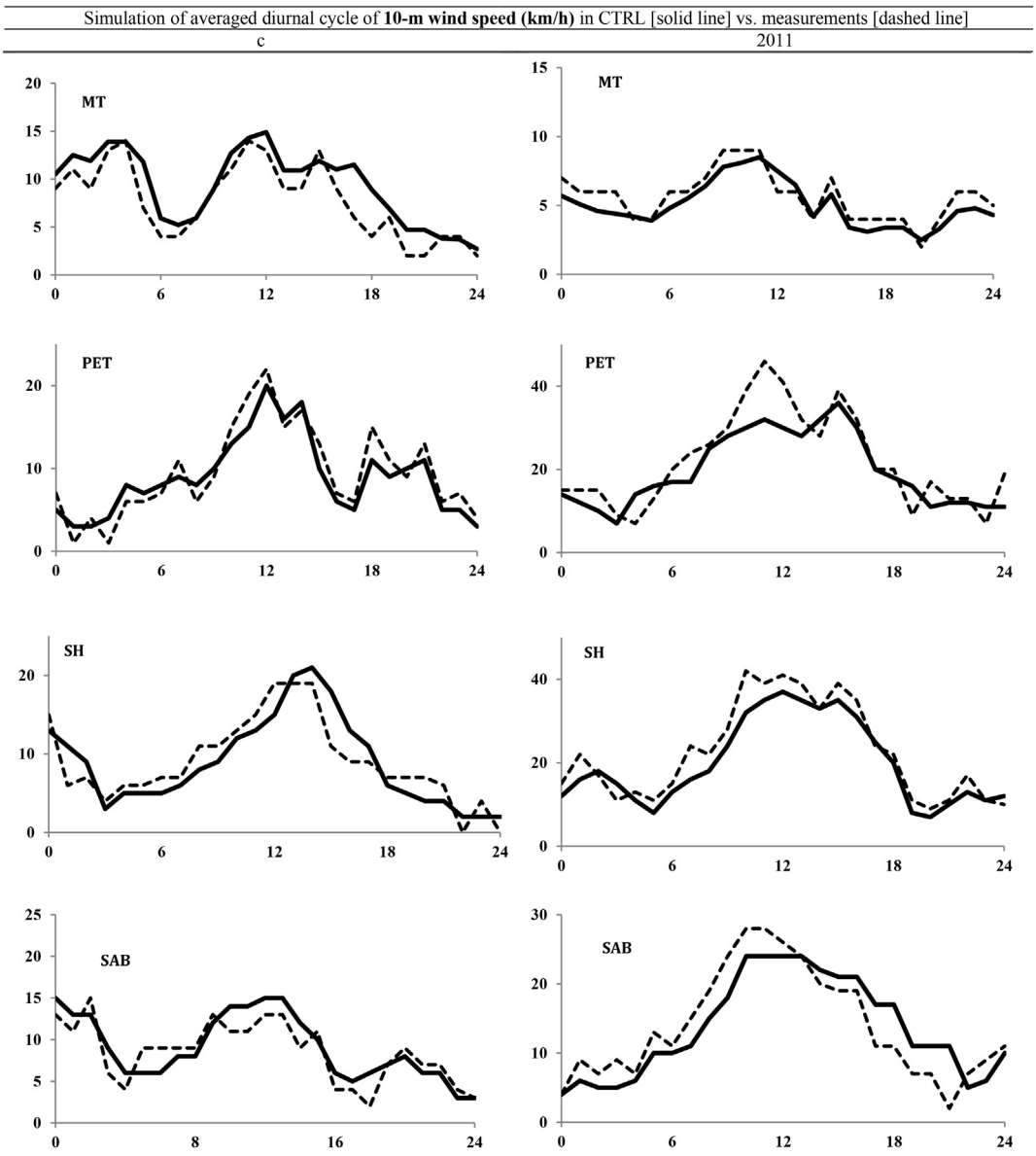

Fig. 2. (*continued*)

3.3. Effects of increasing surface reflectivity

The surface reflectivity of roofs, walls and grounds increased from 0.2 in CTRL scenarios to 0.65, 0.60, and 0.45 in ALBEDO scenarios, respectively. Table 5 represents the averaged 2-m air temperature, 10-m wind speed, 2-m relative humidity and dew point temperature differences between CTRL and ALBEDO scenarios. The averaged 2-m air temperature decreased by 0.8 °C in urban areas (MT and PET) and by 0.4 °C in rural areas (SH and SAB). The simulation results indicate that the T2 reduces less at 12 p.m. compared to 6 p.m. because of the heat that is absorbed by the ground surface during sunlight and then released at sunset and thus added up to the air temperature in the evening. The averaged 10-m wind speed differences between CTRL and ALBEDO scenarios indicate that an increase in surface albedo causes a slight increase in the wind speed in some parts of the domain and a decrease in others. The increase in wind assists the decrease in air temperature in those areas. The averaged 2-m relative humidity differences between these scenarios show a slight increase in relative humidity. The relative humidity increases less in rural areas compared to the urban areas because of more vegetation in rural areas. Fig. 4 shows the daily (3-day) averaged 2-m air temperature, 10-m wind speed, 2-m relative humidity and dew point temperature differences between CTRL and ALBEDO scenarios during these two heat wave periods. Spatially averaged values for urban and rural areas are shown with solid and dashed lines, respectively.

Fig. 5 shows the daily averaged discomfort index (DI) and apparent temperature (AT) for CTRL and ALBEDO scenarios. The results indicate that an increase in surface albedo causes a decrease in apparent temperature and discomfort indices that makes the

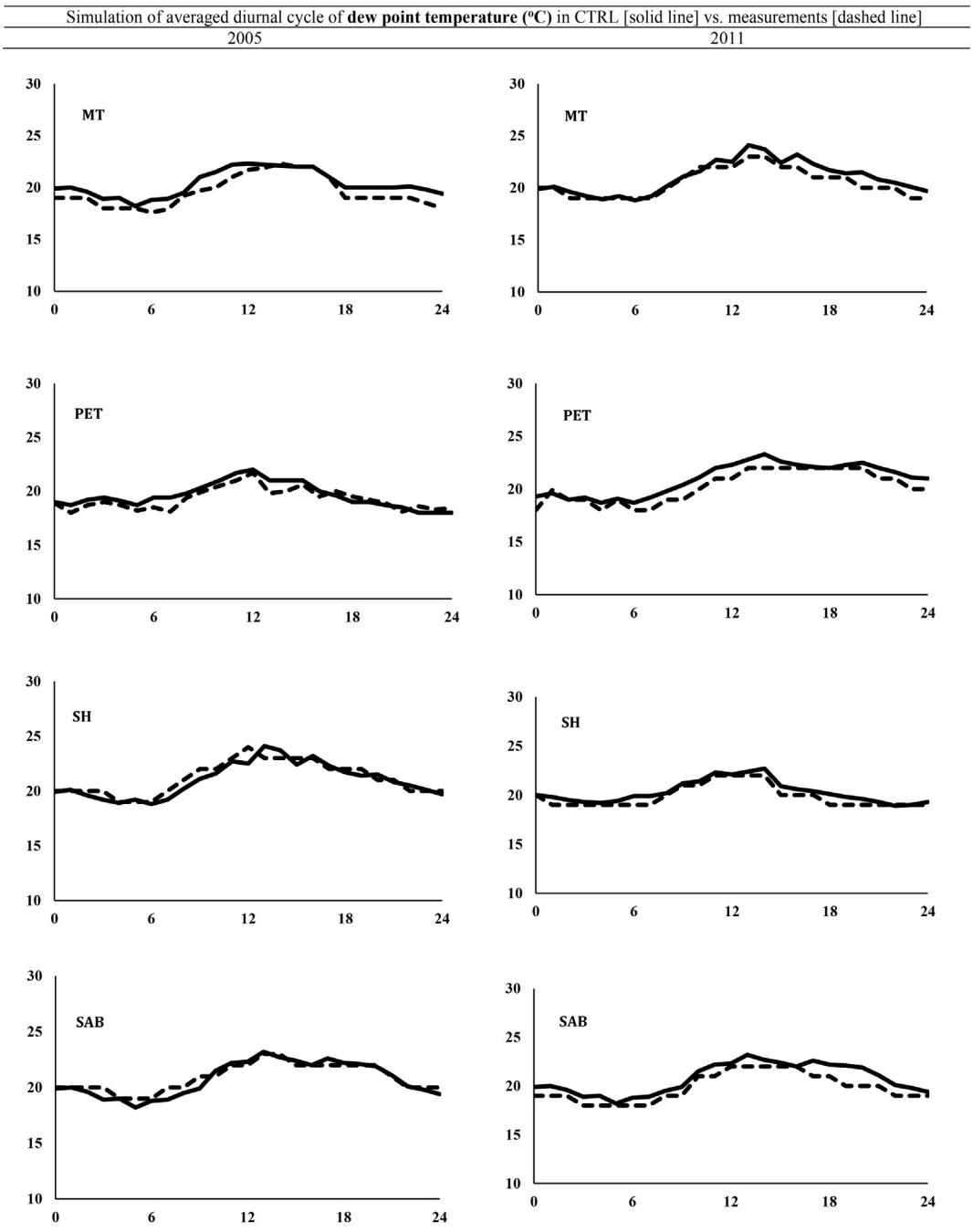

Fig. 2. (*continued*)

environment more preferable and suitable for human beings during summer time and therefore reduces the risk of heat-related morbidity and mortality. We applied two indicators as 2-m air temperature and 2-m relative humidity that extracted from ALBEDO simulation results in these estimations. As the outcomes of increasing surface reflectivity, the DI improved by nearly 3% and 1.7% in urban and rural areas and the AT decreased by nearly 2.6 °C and 1.8 °C in urban and rural areas, respectively. In general, the urban diurnal range of heat indices (HI) is higher than the rural ones; thus, the consequences of increasing surface reflectivity in urban areas are more measurable and obvious than its surroundings.

3.4. Heat-related mortality changes

In Greater Montreal Area, the frequency of dry moderate, moist moderate and moist tropical conditions rank the top three in the

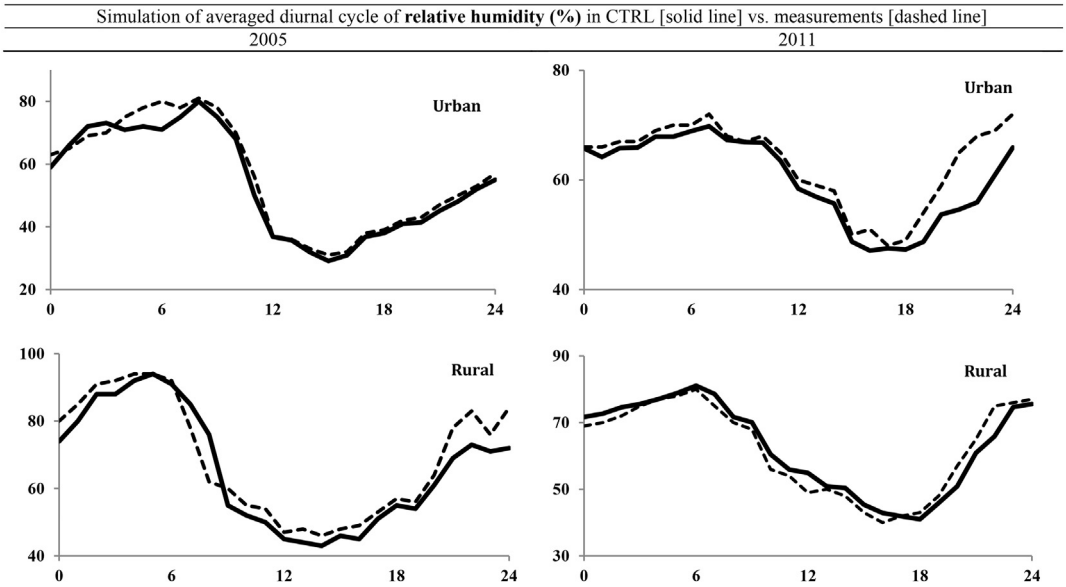

Fig. 2. (*continued*)

spatial synoptic classification in summertime. Three indicators are applied to translate the impacts of extreme heat events intensified by the urban heat island phenomenon and the potential effects of increasing surface reflectivity on heat-related mortality (HRM) rates: air mass type, air temperature and apparent temperature changes for each day during heat-wave event. Here, the mortality related to the oppressive weather types (DT, MT and MT+) because of the heat intensity on a local scale and available data, is estimated based on the Kalkstein et al. (2013) method for the weather conditions in GMA.

The heat-related mortality calculation for dry tropical (DT) that represents the hottest and driest condition is (Eq. (4)):

$$HRM_D = -4.32 + 1.07\mathrm{CD} - 0.066\mathrm{DS} + 0.339\ \mathrm{AT} \tag{4}$$

and for Moist Tropical (MT) and Moist Tropical Plus (MT+) that represent very warm and humid condition is (Eq. (5)):

$$HRM_D = 2.701 - 0.016\mathrm{DS} + 0.339\mathrm{AT} \tag{5}$$

where HRM_D is the estimation of heat-induced mortality on daily basis, CD is consecutive days during heat wave events (day 1 = 1 and day 3 = 3), DS is the day in summer season (JJA) in Montreal (1 = 1st of June and 32 = 1st of July), and AT is apparent temperature in °C at a particular time that consists of humidity and air temperature. We selected the 1600 h local time data to have the full impact of both UHI and extreme heat events on air temperature and humidity.

Increasing surface reflectivity leads to a decrease in air temperature, an increase in relative humidity and dew point temperature, and a slight increase in wind speed. Table 6 represents the 2-m air temperature (T2, (°C)), dew point temperature (DPT, (°C)) and apparent temperature (AT, (°C)) at 1600 h, in CTRL and ALBEDO scenarios. These changes can lead to a significant improvement in human health and comfort and thus reduces heat-related mortality during heat wave events.

We categorized each day into a synoptic air mass classification in the base case and evaluated the impacts of mitigation strategy on SSC. These air mass classifications are based on meteorological changes as air temperature, relative humidity, and wind velocity over the interested domain. Table 7 represents the air mass type for each day during the 2005 and 2011 heat wave periods for CTRL and ALBEDO scenarios. The moist tropical plus air mass type is improved to moist tropical because of the mitigation strategy and surface modification that leads to a decrease in air temperature and an increase in relative humidity. The dry tropical classification has also transformed to dry moderate, which is a more benign condition. These changes cause a decrease in heat-related mortality during these two heat wave events.

Table 8 represents the results of heat-related mortality estimation in CTRL and ALBEDO scenarios. The consequences of surface modifications in urban areas indicate that in the 2005 and 2011 events, there would be 2.7% and 3.7% reduction in heat-related mortality. As the air mass classification shifted from oppressive condition (e.g., DT) to a benign situation (e.g., DM), a reduction in HRM is more noticeable.

4. Discussion

Our simulations show that increasing surface reflectivity decreases urban ambient temperature. The positive impacts of lower temperatures are: (1) improving human health and comfort and (2) decreasing heat-related mortality during heat-wave periods. Decreasing air temperature also has the following positive effects on air quality: (1) a decrease in temperature-dependent rates of certain photochemical reactions (O_3 formation), (2) a decrease in evaporation losses of organic compounds from mobile and stationary sources, and (3) a decrease in cooling energy demands during summer. Human thermal comfort depends on many factors

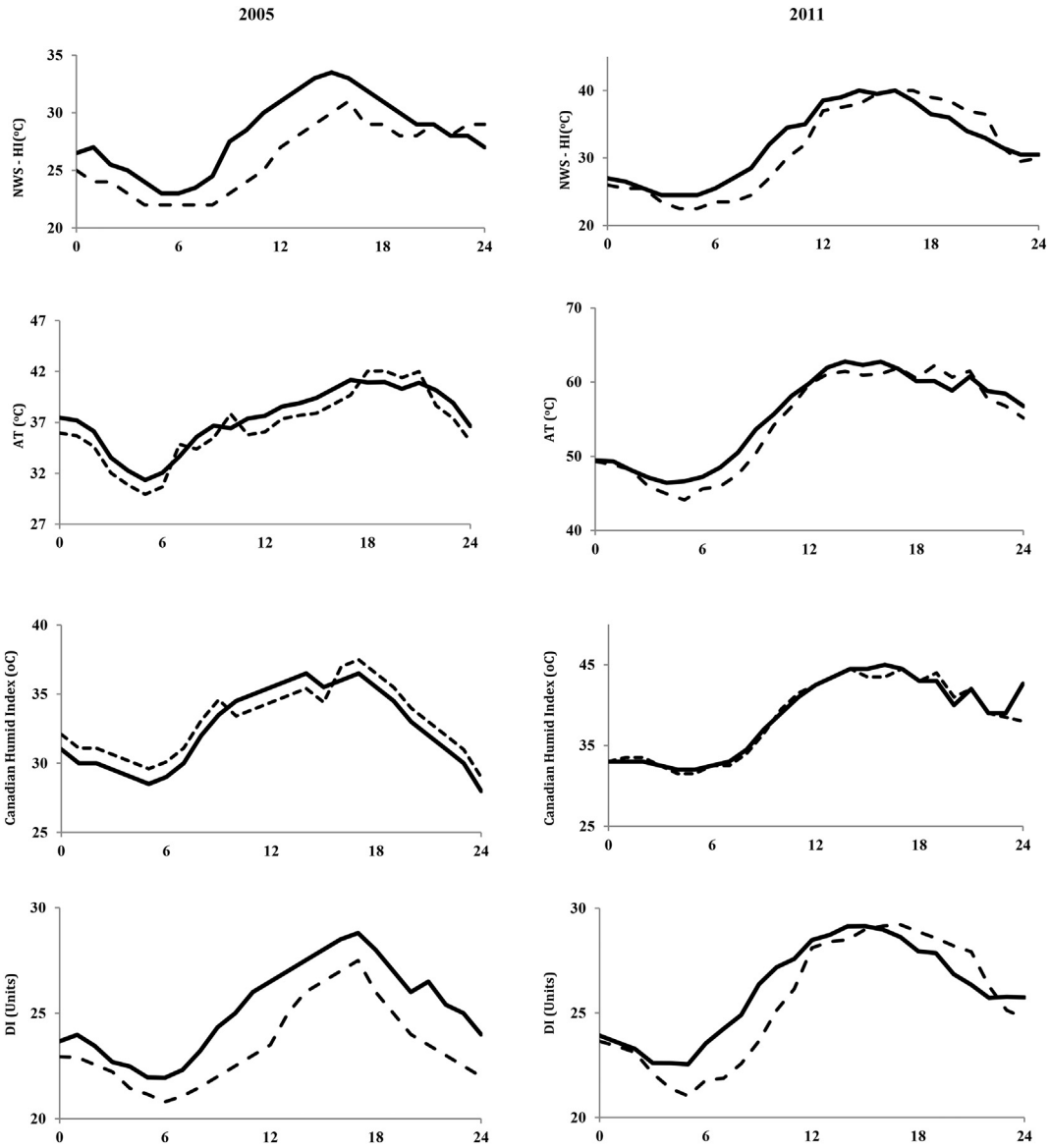

Fig. 3. Simulated averaged diurnal (3-day) cycle of National Weather Service – Heat Index (°C), Apparent Temperature (°C), Canadian Humid Index (°C), Discomfort Index (Units) in CTRL scenarios in 2011 [left] and 2005 [right] shown in urban areas [solid line] and rural areas [dashed line].

Table 5
Averaged 3-day differences of 2-m air temperature(°C), 10-m wind speed(km/h), dew point temperature(°C), and 2-m relative humidity (%) between CTRL and ALBEDO scenarios in GMA during 2005 and 2011 heat wave periods.

CTRL-ALBEDO	Heat-wave	MT	PET	SH	SAB
ΔT2 (°C)	2005	0.7	0. 5	0.2	0.7
	2011	0.8	0.7	0.2	0.6
ΔWS_{10} (km/h)	2005	0.2	−0.05	−0.01	0.01
	2011	0.3	−0.09	−0.02	0.01
ΔDPT(°C)	2005	−0.19	−0.27	−0.18	−0.25
	2011	−0.28	−0.38	−0.13	−0.29
ΔRH_2 (%)	2005	−0.4	−0.2	−0.09	−0.13
	2011	−0.3	−0.4	−0.17	−0.11

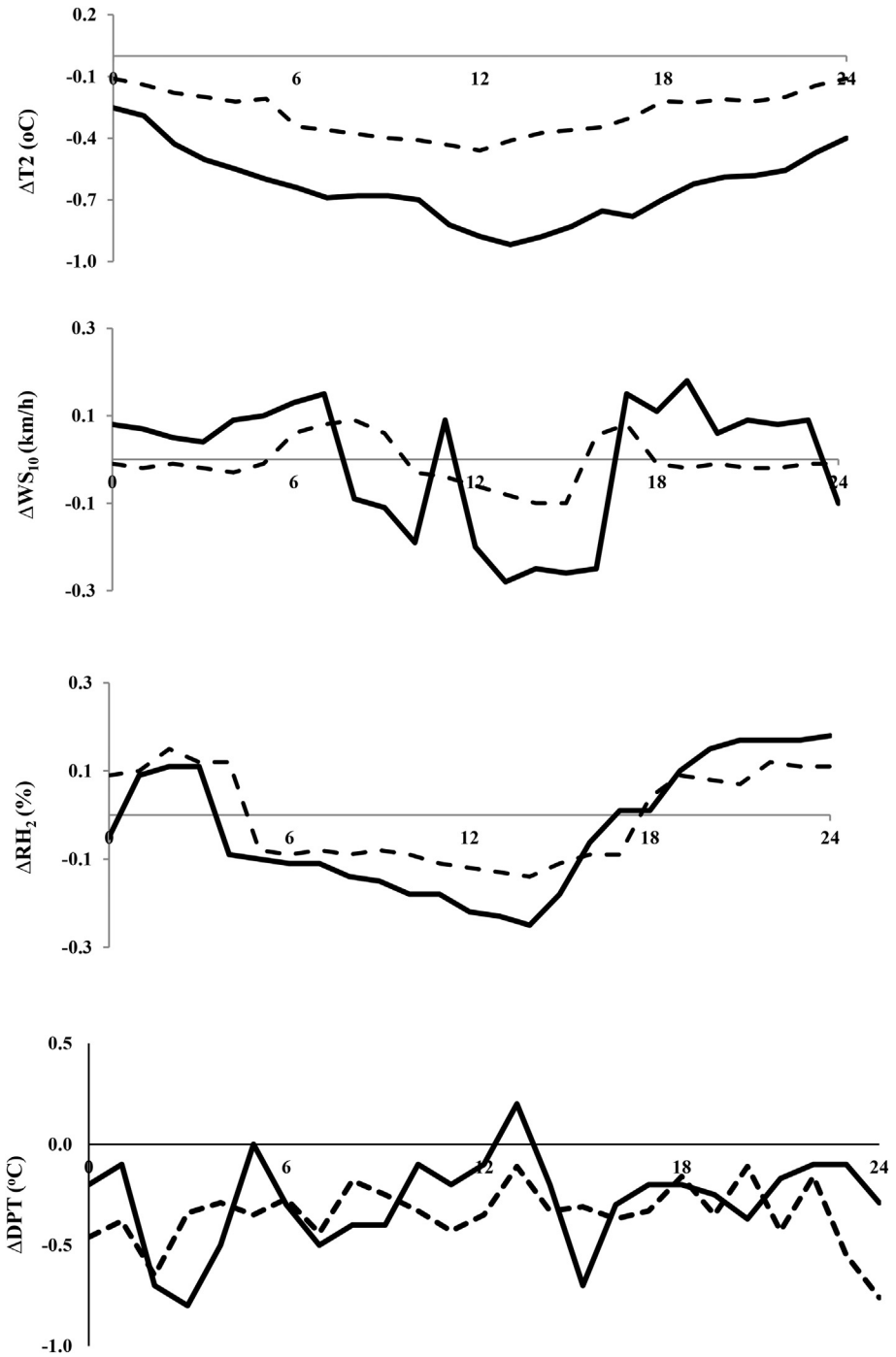

Fig. 4. Daily averaged 2-m air temperature (°C), 10-m wind speed (km/h), dew point temperature (°C), and 2-m relative humidity (%) and differences between CTRL and ALBEDO in GMA during 2005 & 2011 heat wave period. Spatially averaged values for urban and rural areas are shown with solid and dashed line, respectively.

such as air temperature, humidity, wind speed, radiant temperature, metabolic rates, clothing levels and each individual physiology and states. Here, we focused on the first three factors that also affect the heat-related mortality directly and disregarded others which are mostly concerning the human thermal comfort.

There are some factors that affect heat-related mortality that are not considered in our analyses. The effects of a decrease in ambient temperature on HRM is evaluated, whereas the rate of mortality is not necessarily related to outside temperature. The effects of cool roofs on indoor temperature and its positive impacts on human comfort and indoor heat related mortality has not been

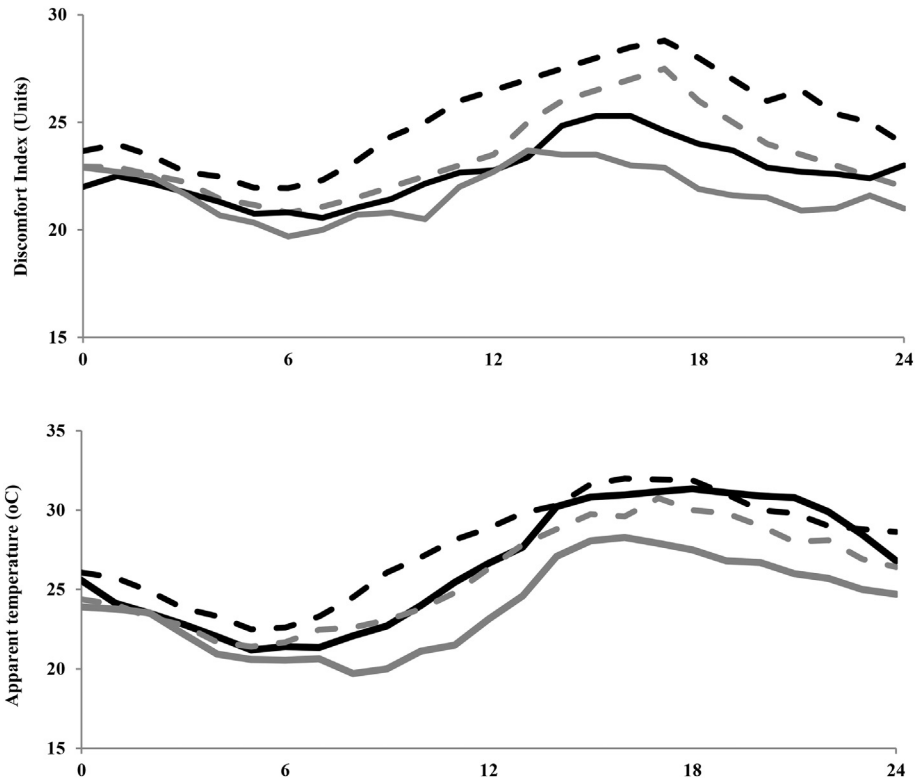

Fig. 5. Daily averaged discomfort index (Units) and apparent temperature (°C) shown in CTRL [dashed line] and ALBEDO [solid line] scenarios during 2005 & 2011 heat wave period for urban [black line] and rural [grey line] areas.

Table 6
2-m air temperature (T2, (°C)), dew point temperature (DPT, (°C)), and apparent temperature (AT, (°C)) at 1600 h, in CTRL and ALBEDO scenarios during 2005 & 2011 heat wave events in GMA.

Averaged variables	CTRL Scenario			ALBEDO Scenario		
	T2 (°C)	DPT (°C)	AT (°C)	T2 (°C)	DPT (°C)	AT (°C)
10-Jul-2005	29.4	22.5	32.2	28.5	22.7	31.9
11-Jul-2005	32.4	20.9	35.3	31.4	21.3	34.2
12-Jul-2005	31.7	21.8	34.8	30.8	22.1	34.1
Event Average	31.6	21.7	34.1	30.2	22.1	33.3
21-Jul-2011	32.9	22.3	35.4	32.2	22.5	35.2
22-Jul-2011	31.7	23.2	34.8	30.9	23.6	34.2
23-Jul-2011	31.2	20.6	35.2	29.4	20.9	32.2
Event Average	31.9	22.0	35.1	30.8	22.4	33.8

Table 7
Air mass classifications on each day during 2005 & 2011 heat wave periods in GMA, the bold entries show changes in air mass type resulted in increasing surface albedo.

Scenario	CTRL	ALBEDO
10-Jul-2005	DT	DT
11-Jul-2005	**MT+**	**MT**
12-Jul-2005	DT	DT
21-Jul-2011	**MT+**	**MT**
22-Jul-2011	MT	MT
23-Jul-2011	**DT**	**DM**

Table 8
Daily heat-related mortality estimation based on above calculations for DT, MT and MT+ during the 2005 & 2011 heat wave periods. For human lives, the numbers are shown with 1 decimal.

Mortality estimations		
Scenario	CTRL	ALBEDO
10-Jul-2005	4.9	4.8
11-Jul-2005	13.9	13.6
12-Jul-2005	7.8	7.6
Total HRM	~ 27	~ 26
Average Mortality	8.9	8.7
Averaged reduction (%)		**2.7%**
21-Jul-2011	13.9	13.8
22-Jul-2011	13.6	13.4
23-Jul-2011	7.3	6.2
Total HRM	~ 35	~ 33
Average Mortality	11.6	11.2
Averaged reduction (%)		**3.7%**

investigated. Other factors as age, gender, economic and educational level of the society have not been accounted for. Current and previous health issues that would be more affected during heatwave periods and lead to death, has not been included. The consequences of heatwave on air quality and ozone production have not been considered. Here, we focused on four heat stress indices: National Weather Service – Heat Index (NWS-HI), Apparent Temperature (AT), Canadian Humid Index (CHI), and Discomfort Index (DI) to estimate the thermal comfort. The solar radiation loads and wet bulb global temperature (WBGT) are factors that need to be estimated concerning human thermal comfort (Epstein and Moran, 2006), which are not considered in this study.

Our simulations and analyses are based on the assumptions that (1) the population density and urban structure over the domain is homogenous, (2) other parameters apart from temperature, humidity and wind speed have minimal effects on UHI phenomenon, heatwave events and heat-related mortality, (3) changes on air mass classification during summer is based on previous studies during 20 years in GMA, (4) the results are based on three consecutive days during heatwave events (but the simulation of the entire summer or even a year is required to achieve a more definite conclusion), (5) the effects of air quality on HRM is negligible, and (6) the effects of air conditioning in the buildings on HRM are the same in both CTRL and ALBEDO cases.

Three of the six heat wave days presented air mass changes from more to less oppressive conditions. The results are somewhat similar to other studies. Kalkstein et al. (2013) showed that the UHI mitigation strategies in the District of Columbia led to the air mass type changes on two of the four heatwave events. These changes contribute to a 7% reduction in the total number of heat-related mortality. They conducted additional research in the District of Columbia in 2011, during a 10-year period and demonstrated that 11% of summer days in this area experience the oppressive air mass type that will be modified to more benign ones by increasing surface albedo (Kalkstein et al., 2013). We limited our study to the effects of increasing surface reflectivity on heat-related mortality. However, there is no one strategy that can fit all the needs of a city. Mitigation strategies need to be region specific and the installation and implementation of cool surfaces need to be evaluated based on urban morphology, building layout patterns, trees arrangements, and wind speed and distribution.

Kalkstein et al. (2013) investigated the effects of UHI mitigation strategies on health-debilitation air masses in four cities across the US. The results of increasing albedo and vegetation indicated that the air mass type changed by an average of 7%, 16%, 3% and 4% in Detroit, Los Angeles, New Orleans and Philadelphia, respectively. The heat-related death decreased by an average of 5 to 10% in these cities. The results of another study by Kalkstein (1999) showed that a 1-2 °C reduction in outdoor temperature, along with some other meteorological changes, could reduce mortality by 10–20%. Here, the ratio of 50% positive modification in air mass classifications is similar to EPA study (Kalkstein and Sheridan, 2003). Our results indicating an average of 3.2% reduction in heat-related mortality during the 2005 and 2011 heat wave period in GMA (a 2.7% reduction in HRM in the 2005 heat wave period and a 3.7% reduction in the 2011 heat wave period), corroborate with EPA-sponsored studies on cool cities (Kalkstein and Sheridan, 2003; Vanos et al., 2013, 2014; Sheridan and Kalkstein, 2004; Sheridan et al., 2009). According to Canadian Environmental Health Atlas (CEHA 2018), 121 people die every year in Montreal because of heat related issues; a 3.2% reduction becasuse of albedo increase in GMA, could save 4 lives per year. Itn another study carried out by Bustinza et al. (2013) for Quebec, Canada, the number of heat-related death in GMA (including Montreal, Laval, Monteregie, and Lanaudiere with the total population of 4,221,002) was estimtaed to be 209 people during July 2010 heat wave period alone. A 3.2% reduction in HRM would results in savings life of 6 people during that period.

5. Summary and conclusions

The main objective of this study was to investigate the effects of increasing surface reflectivity on heat-related mortality in Greater Montreal Area during two heat wave periods in 2005 and 2011. Numerical simulations were conducted using the online Weather Research and Forecasting model (WRFV3.6.1) coupled with a multi-layer of the Urban Canopy Model (ML-UCM). The simulation

results were analysed in terms of four meteorological parameters: 2-m air temperature, 10-m wind speed, 2-m relative humidity, dew point temperature and four heat stress indices: National Weather Service – Heat Index, apparent temperature, Canadian Humid Index, and Discomfort Index. We employed a series of metrics calculations to evaluate model performance and compared the simulation results with the measurements obtained from four weather stations over the domain. The comparisons of the base case simulations indicated that the model on average slightly overestimates the meteorological variables.

The albedo of roofs, walls and grounds were increased from 0.2 in CTRL scenarios to 0.65, 0.60, and 0.45 in ALBEDO scenarios, respectively. The results showed that the differences between meteorological parameters (T2, WS10, RH2, DPT) in CTRL and ALBEDO scenarios are more significant in urban areas than its surroundings. The average daily 2-m air temperature reduced by 0.8 °C in urban areas during both heat wave events, whereas this amount in rural area was around 0.4 °C. The albedo enhancement caused a slight increase in wind speed in urban areas that increase the convection heat transfer and thus decrease the skin temperature. A higher wind speed reduces the effects of heat and ambient temperature and produces a more pleasant condition. The results showed an increase in relative humidity and dew point temperature by nearly 2%. The relative humidity changes are less obvious in rural areas compared to the urban areas because of the existence of more vegetation spaces, and thus moisture in the region. The effects of increasing albedo have also been investigated on four indices of heat stress. The results showed that since surface albedo modifications reduced temperature and increased relative humidity, these indices were also modified and improved to some extent. Increasing surface albedo is a verifiable strategy to mitigate the UHI effects. It should be noted that this strategy is a region specific and needs to be evaluated over any interested area because it depends on urban characteristics and morphology.

Here, three indicators are applied to translate the effects of extreme heat events and the potential of increasing surface reflectivity on heat-related mortality rates: air mass type, air temperature and apparent temperature changes for each day during heat-wave periods. As the consequences of ISR, the moist tropical plus and dry tropical air mass types are shifted to moist tropical and dry moderate, respectively. These changes cause a decrease in heat-related mortality during these two heat wave events. Three of the six heat wave days showed air mass changes from more to less oppressive conditions. The beneficial outcome is a reduction in heat-related death by approximately 3.2% during heat wave periods, meaning that 4-6 lives per year could be saved. It should be noted that by reducing ambient temperature, the pollutants emission from biogenic and anthropogenic sources and thus photochemical reaction rates will reduce. So, the death related to air quality will also reduce. In addition, increasing surface reflectivity shift days into less oppressive air masses by 50%.

The heat-related mortality estimation is based upon some assumptions and limitations. The effects of air pollution as ozone concentrations because of elevated heat is neglected. The impacts of wind speed and radiation budget changes as meteorological parameters and human physical characteristics, such as age, gender, economic and educational status, have not been taken into account. Hence, the effects of these accumulation factors are required to be considered in future studies. While it appears unlikely that increasing surface reflectivity contributes to large reductions in ambient temperature in urban areas (as 2 °C or greater), the study shows that cooling temperature to even less than a degree can lead to air mass category changes, reduce the adverse effects of elevated temperature in urban areas, thus improving human comfort and decreasing heat-related mortality to some noticeable extent.

Acknowledgment

The funding for this research provided by the National Science and Engineering Research Council of Canada under discovery program.

References

Akbari, H., Kolokotsa, D., 2016. Three decades of urban heat islands and mitigation technologies research. Enbuild 133, 834–842.
Akbari, H., Touchaei, A.G., 2014. Modeling and labeling heterogeneous directional reflective roofing materials. Sol. Energy Mater. Sol. Cells 124, 192–210.
Akbari, H., Pomerantz, M., Taha, H., 2001. Cool surfaces and shade trees to reduce energy use and improve air quality in urban areas. Sol. Energy 70 (3), 295–310.
Akbari, H., Menon, S., Rosenfeld, A., 2009. Global cooling: increasing world-wide urban albedos to offset CO2. Clim. Chang. 94 (3–4), 275–286.
Anderson, B.G., Bell, M.L., 2009. Weather-related mortality: how heat, cold, and heat waves affect mortality in the United States. Epidemiology 20 (2), 205–213.
Arnfield, A.J., 2003. Two decades of urban climate research: a review of turbulence, exchanges of energy and water, and the urban heat island. Int. J. Climatol. 23, 1–26.
Åström, D.O., Forsberg, B., Rocklöv, J., 2011. Heat wave impact on morbidity and mortality in the elderly population: a review of recent studies. Maturitas 69 (2), 99–105.
Ban-Weiss, G.A., Woods, J., Levinson, R., 2014. Using remote sensing to quantify albedo of roofs in seven California cities, part 1: methods. Sol. Energy 115, 777–790.
Barnett, A.G., Tong, S., Clements, A.C., 2010. What measure of temperature is the best predictor of mortality? Environ. Res. 110 (6), 604–611.
Basu, R., 2009. High ambient temperature and mortality: a review of the epidemiologic studies from 2001 to 2008. Environ. Health 8, 40–48.
Basu, R., Samet, J.M., 2002. Relation between elevated ambient temperature and mortality: a review of the epidemiologic evidence. Epidemiol. Rev. 24 (2), 190–202.
Bunker, A., Wildenhain, J., Vandenbergh, A., Henschke, N., Rocklöv, J., Hajat, S., Sauerborn, R., 2016. Effects of air temperature on climate-sensitive mortality and morbidity outcomes in the elderly; a systematic review and meta-analysis of epidemiological evidence. EBioMedicine 6, 258–268.
Bustinza, R., Lebel, G., Gosselin, P., Belanger, D., Chebana, F., 2013). Health impacts of the July 2010 heat wave in Québec, Canada. BMC Public Health 13, 56. http://dx.doi.org/10.1186/1471-2458-13-56.
Canadian Environmental Health Atlas, 2018. Canadian Environmental Health Atlas. visited 20 June 2018. http://www.ehatlas.ca/climate-change/heat-waves.
Chen, F., Dudhia, J., 2001. Coupling an advanced land surface–hydrology model with the Penn State–NCAR MM5 modeling system. Part I: model implementation and sensitivity. Mon. Weather Rev. 129, 569–585.
Chen, F., Kusaka, H., Bornstein, R., Ching, J., Grimmond, C.S.B., Grossman-Clarke, S., Loridan, T., Manning, K.W., Martilli, A., Miao, S., Sailor, D., Salamanca, F.P., Taha, H., Tewari, M., Wang, X., Wyszogrodzkia, A.A., Zhang, C., 2011. The integrated WRF/urban modelling system: development, evaluation, and applications to urban environmental problems. Int. J. Climatol. 31, 273–288.
Conti, S., Meli, P., Minelli, G., Solimini, R., Toccaceli, V., Vichi, M., Beltrano, C., Perini, L., 2005. Epidemiologic study of mortality during the summer 2003 heat wave in Italy. Environ. Res. 98 (3), 390–399.

Csiszar, I., Gutman, G., 1999. Mapping global land surface albedo from NOAA AVHRR. J. Geophys. Res. 104, 6215–6228.
Cusack, L., de Crespigny, C., Athanasos, P., 2011. Heatwaves and their impact on people with alcohol, drug and mental health conditions: a discussion paper on clinical practice considerations. J. Adv. Nurs. 67 (4), 915–922.
Diaz, J., Jordan, A., García, R., Lopez, C., Alberdi, J., Hernandez, E., Otero, A., 2002. Heat waves in Madrid 1986-1997: effects on the health of the elderly. Int. Arch. Occup. Environ. Health 75 (3), 163–170.
Diffenbaugh, N.S., Ashfaq, M., 2010. Intensification of hot extremes in the United States. Geophys. Res. Lett. 37 (15), 157–185.
Environment Canada, 2017. Online. http://climate.weather.gc.ca/historical_data/search_historic_data_e.html.
Epstein, Y., Moran, D.S., 2006. Thermal comfort and heat stress indices. Ind. Health 44 (3), 388–398.
Fischer, E.M., Oleson, K.W., Lawrence, D.M., 2012. Contrasting urban and rural heat stress responses to climate change. Geophys. Res. Lett. 39 (3).
Gilliam, R.C., Hogrefe, C., Rao, S.T., 2006. New methods for evaluating meteorological models used in air quality applications. Atmos. Environ. 40, 5073–5086.
Grell, G.A., Devenyi, D., 2002. A generalized approach to parameterizing convection combining ensemble and data assimilation techniques. Geophys. Res. Lett. 29 (14), 31–38.
Hajat, S., O'Connor, M., Kosatsky, T., 2010. Health effects of hot weather: from awareness of risk factors to effective health protection. Lancet 375 (9717), 856–863.
Hanna, A.F., Yeatts, K.B., Xiu, A., Zhu, Z., Smith, R.L., 2011. Associations between ozone and morbidity using the spatial synoptic classification system. Environ. Health 10 (1), 1–15.
Harlan, S.L., Ruddell, D.M., 2011. Climate change and health in cities: impacts of heat and air pollution and potential co-benefits from mitigation and adaptation. Curr. Opin. Environ. Sustain. 3 (3), 126–134.
Harlan, S.L., Brazel, A.J., Prashad, L., Stefanov, W.L., Larsen, L., 2006. Neighborhood microclimates and vulnerability to heat stress. Soc. Sci. Med. 63 (11), 2847–2863.
Hong, B., Lin, B., 2014. Numerical study of the influences of different patterns of the building and green space on microscale outdoor thermal comfort and indoor natural ventilation. Build. Simul. 7, 525–536.
Horton, D.E., Skinner, C.B., Singh, D., Diffenbaugh, N.S., 2014. Occurrence and persistence of future atmospheric stagnation events. Nat. Clim. Change Lett. 4, 698–703.
Sherwood, S.C., Huber, M., 2010. An adaptability limit to climate change due to heat stress. Proc. Natl. Acad. Sci. U. S. A. 107, 9552–9555.
Iacono, M.J., Delamere, J.S., Mlawer, E.J., Shephard, M.W., Clough, S.A., Collins, W.D., 2008. Radiative forcing by longelived greenhouse gases: calculations with the AER radiative transfer models. J. Geophys. Res. 113 (131-03).
IPCC, 2014. Summary for policymakers. In: Climate Change 2014 (Ed.), Impacts, Adaptation, and Vulnerability. Part A: Global and Sectoral Aspects. Contribution of Working Group II to the Fifth Assessment Report of the Intergovernmental Panel on Climate Change, pp. 1–32 (New York (NY), USA).
Jacobson, M., Ten Hoeve, J.E., 2012. Effects of urban surfaces and white roofs on global and regional climate. J. Clim. 25, 1–28.
Jandaghian, Z., Akbari, H., 2018. The effects of increasing surface albedo on urban climate and air quality: adetailed study for Sacramento, Houston, and Chicago. Climate 6 (2), 19.
Jandaghian, Z., Touchaei, G.A., Akbari, H., 2018. Sensitivity analysis of physical parameterizations in WRF for urban climate simulations and heat island mitigation in Montreal. Urban Clim. 24, 577–599.
Janjic, Z.I., 1994. The step–mountain eta coordinate model: further developments of the convection, viscous sublayer, and turbulence closure schemes. Mon. Weather Rev. 122, 927–945.
Janjic, Z.I., 2002. Nonsingular implementation of the Mellor–Yamada Level 2.5 Scheme in the NCEP meso model. In: NCEP Office Note, No. 437.
Jenkins, K., Hall, J., Glenis, V., Kilsby, C., Mccarthy, C., Goodess, D., Smith, N., Malleson, M., 2014. Probabilistic spatial risk assessment of heat impacts and adaptations for London. Clim. Change 124, 105–117.
Kalkstein, L.S., 1999. A new approach to evaluate the impact of climate on human mortality. Environ. Health Perspect. 96, 145.
Kalkstein, L.S., Sheridan, S.C., 2003. The impact of heat island reduction strategies on health-debilitating oppressive air masses in urban areas. In: Phase 1. U.S. EPA Heat Island Reduction Initiative.
Kalkstein, L.S., Valimont, K.M., 1986. An evaluation of summer discomfort in the United States using a relative climatological index. Bull. Am. Meteorol. Soc. 67, 842–848.
Kalkstein, L.S., Greene, J.S., Mills, D., Samenow, J., 2011. An evaluation of the progress in reducing heat- related human mortality in major U.S. cities. Nat. Hazards 56, 113–129.
Kalkstein, L., Sailor, D., Shickman, K., Sherdian, S., Vanos, J., 2013. Assessing the Health Impacts of Urban Heat Island Reduction Strategies in the District of Columbia. In: Report DDOE ID#2013-10-OPS, Global Cool Cities Alliance.
Kruger, E.L., Minella, F.O., Rasia, F., 2010. Impact of urban geometry on outdoor thermal comfort and air quality from field measurements in Curitiba, Brazil. Build. Environ. 46, 621–634.
Lin, Y., Colle, B.A., 2011. A new bulk microphysical scheme that includes riming intensity and temperature–dependent ice characteristics. Mon. Weather Rev. 139, 1013–1035.
Lin, Y., Farley, R., Orville, H.D., 1983. Bulk parameterization of the snow field in a cloud model. Clim. Appl. Meteorol. 22, 1065–1092.
Liu, X.-H., Zhang, Y., Olsen, K., Wang, W.-X., Do, B., Bridgers, G., 2010. Responses of future air quality to emission controls over North Carolina—Part I: Model evaluation for current-year simulations. Atmos. Environ. 44, 2443–2456.
Martel, B., Giroux, J.X., Gosselin, P., Chebana, F., Ouarda, T.B.M.J., Charron, C., 2010. Indicateurs et seuils météorologiques pour les systèmes de veille-avertissement lors de vagues de chaleur au Québec. Institut national de santé publique du Québec, Québec ISBN 978-2-550-59896-1.
Matzarakis, A., Nastos, P.T., 2011. Human-biometeorological assessment of heat waves in Athens. Theor. Appl. Climatol. 105, 99–106.
Mcgeehin, M.A., Mirabelli, M., 2001. The potential impacts of climate variability and change on temperature-related morbidity and mortality in the United States. Environ. Health Perspect. 109 (Suppl. 2), 185–189.
Mcmichael, A., Woodruff, R.E., Hales, S., 2006. Climate change and human health: present and future risks. Lancet 367 (9513), 859–869.
Mesinger, F., Dimego, G., Kalnay, E., Mitchell, K., Shafran, P.C., Ebisuzaki, W., Jovic, D., Woollen, J., Rogers, E., Berbery, E.H., Ek, M.B., Fan, Y., Grumbine, R., Higgins, W., Li, H., Lin, Y., Manikin, G., Parrish, D., Shi, W., 2006. North American regional reanalysis. Bull. Am. Meteorol. Soc. 87 (3), 343–360.
Nitschke, M., Tucker, G.R., Hansen, A., Williams, S., Zhang, Y., Bi, P., 2011. Impact of two recent extreme heat episodes on morbidity and mortality in Adelaide, South Australia: a case-series analysis. Environ. Health 10 (42), 10–42.
Oleson, K.W., Bonan, G.B., Feddema, J., 2010. The effects of white roofs on urban temperature in a global climate model. Geophys. Res. Lett. 37 (37), 03–21.
Oliver, B., Hoelscher, M.T., Meier, F., Nehls, T., Ziegler, F., 2015. Evaluation of the health-risk reduction potential of countermeasures to urban heat islands. Enbuild 114, 27–37.
O'Neill, M.S., Ebi, K.L., 2009. Temperature extremes and health: impacts of climate variability and change in the United States. J. Occup. Environ. Med. 51, 13–25.
O'Neill, M.S., Zanobetti, A., Schwartz, J., 2003. Modifiers of the temperature and mortality association in seven US cities. Am. J. Epidemiol. 157, 1074–1082.
O'Neill, M.S., Zanobetti, A., Schwartz, J., 2005. Disparities by race in heat-related mortality in four US cities: the role of air conditioning prevalence. J. Urban Health Bull. N.Y. Acad. Med. 82, 191–197.
Peng, R.D., Bobb, J.F., Tebaldi, C., Mcdaniel, L., Bell, M.L., Dominici, F., 2011. Toward a quantitative estimate of future heatwave mortality under global climate change. Environ. Health Perspect. 119 (5), 701–706.
Sheridan, S.C., 2002. The redevelopment of a weather-type classification scheme for North America. Int. J. Climatol. 22 (1), 51–68.
Sheridan, S.C., Kalkstein, L.S., 2004. Progress in heat watch-warning system technology. Bull. Am. Meteorol. Soc. 85, 1931–1941.
Sheridan, S., Kalkstein, A., Kalkstein, L., 2009. Trends in heat-related mortality in the United States, 1975–2004. Nat. Hazards 50 (1), 145–160.
Skamarock, W.C., Klemp, J.B., Dudhia, J., Gill, D.O., Barker, D.M., Duha, M.G., Huang, X.Y., Wang, W., Powers, J.G., 2008. A Description of the Advanced Research WRF Version 3. National Center for Atmospheric Research, Boulder, CO, USA.
Smoyer, K.E., Rainham, D.G., Hewko, J.N., 2000. Heat-stress-related mortality in five cities in southern Ontario: 1980–1996. Int. J. Biometeorol. 44, 190–197.

Taha, H., 1997. Urban climates and heat islands: albedo, evapotranspiration, and anthropogenic heat. Energy Build. Spec. Issue Urban Heat Islands 25, 99–103.
Taha, H., 2008. Urban surface modification as a potential ozone air-quality improvement strategy in California: a mesoscale modeling study. Bound. Layer Meteorol. 127, 219–239.
Taha, H., 2009. Mesoscale and Meso-Urban Meteorological and Photochemical Modeling of Heat Island Mitigation in California: Results and Regulatory Aspects Conference on Countermeasures to UHI, Berkeley (CA) USA.
Touchaei, A.G., Akbari, H., 2013. The climate effects of increasing the albedo of roofs in a cold region. Adv. Build. Energy Res. 7, 186–191.
Touchaei, A.G., Akbari, H., 2015. Evaluation of the seasonal effect of increasing albedo on urban climate and energy consumption of buildings in Montreal. Urban Clim. 14, 278–289.
Vandentorren, S., Bretin, P., Zeghnoun, A., Mandereau-Bruno, L., Croisier, A., Cochet, C., Riberon, J., Siberan, I., Declercq, B., Ledrans, M., 2006. Heat-related mortality e august 2003 heat wave in France: risk factors for death of elderly people living at home. Eur. J. Pub. Health 16 (6), 583–591.
Vaneckova, P., Beggs, P.J., Jacobson, C.R., 2010. Spatial analysis of heat-related mortality among the elderly between 1993 and 2004 in Sydney, Australia. Soc. Sci. Med. 70 (2), 293–304.
Vanos, J.K., Cakmak, S., Bristow, C., Brion, V., Tremblay, N., Martin, S.L., Sheridan, S.S., 2013. Synoptic weather typing applied to air pollution mortality among the elderly in 10 Canadian cities. Environ. Res. 126, 66–75.
Vanos, J.K., Hebbern, C., Cakmak, S., 2014. Risk assessment for cardio- vascular and respiratory mortality due to air pollution and synoptic meteorology in 10 Canadian cities. Environ. Pollut. 185, 322–332.
Wang, K., Zhang, Y., Jang, C.J., Phillips, S., Wang, B.Y., 2009. Modelling study of intercontinental air pollution transport over the trans-Pacific region in 2001 using the community multiscale air quality (CMAQ) modelling system. J. Geophys. Res. 114 (43-07).
Wang, X.Y., Barnett, A.G., Yu, W., Fitzgerald, G., Tippett, V., Aitken, P., Neville, G., Mcrae, D., Verrall, K., Tong, S., 2012. The impact of heatwaves on mortality and emergency hospital admissions from non-external causes in Brisbane, Australia. Occup. Environ. Med. 69 (3), 163–169.
World Health Organization (WHO), 2010. International Classification of Diseases, 10th Revision (ICD-10).
WRF User's Guide, 2016. Mesoscale & Microscale Meteorology Division. National Center for Atmospheric Research (NCAR).
Wu, S.-Y., Krishnan, S., Zhang, Y., Aneja, V., 2008. Modelling atmospheric transport and fate of ammonia in North Carolina, part I. Evaluation of meteorological and chemical predictions. Atmos. Environ. 42, 3419–3436.
Yardley, J., Sigal, R.J., Kenny, G.P., 2011. Heat health planning: the importance of social and community factors. Glob. Environ. Change 21 (2), 670–679.
Zanobetti, A., Schwartz, J., 2008. Temperature and mortality in nine US cities. Epidemiology 19, 563–570.
Zanobetti, A., Luttmann-Gibson, H., Horton, E.S., Cohen, A., Coull, B.A., Hoffmann, B., Schwartz, J.D., Mittleman, M.A., Li, Y., Stone, P.H., de Souza, C., Lamparello, B., Koutrakis, P., Gold, D.R., 2014. Brachial artery responses to ambient pollution, temperature, and humidity in people with type 2 diabetes: a repeated- measures study. Environ. Health Perspect. 122 (3), 242.
Zhang, K., Li, Y., Schwartz, J.D., O'Neill M.S., 2014a. What weather variables are important in predicting heat-related mortality? A new application of statistical learning methods. Environ. Res. 132, 350–359.
Zhang, K., Chen, Y.H., Schwartz, J.D., Rood, R.B., O'Neill, M.S., 2014b. Using forecast and observed weather data to assess performance of forecast products in identifying heat waves and estimating heat wave effects on mortality. Environ. Health Perspect. 122, 912–918.